How to cite: *Angew. Chem. Int. Ed.* **2022,** *61,* e202211747
International Edition: doi.org/10.1002/anie.202211747
German Edition: doi.org/10.1002/ange.202211747

VIP **Excited States** **Very Important Paper**

# The Excited-State Creutz–Taube Ion

*German E. Pieslinger, Ivana Ramírez-Wierzbicki, and Alejandro Cadranel**

**Abstract:** The excited-state version of the Creutz–Taube ion was prepared via visible light excitation of $[(NH_3)_5Ru^{II}(\mu\text{-pz})Ru^{II}(NH_3)_5]^{4+}$. The resulting excited state is a mixed valence $\{Ru^{III-\delta}(\mu\text{-pz}^{\bullet-})Ru^{II+\delta}\}$ transient species, which was characterized using femtosecond transient absorption spectroscopy with vis-NIR detection. Very intense photoinduced intervalence charge transfers were observed at 7500 $cm^{-1}$, revealing an excited-state electronic coupling element $H_{DA}$ = 3750 $cm^{-1}$. DFT calculations confirm a strongly delocalized excited state. A notable consequence of strong electron delocalization is the nanosecond excited state lifetime, which was exploited in a proof-of-concept intermolecular electron transfer. The excited-state Creutz–Taube ion is established as a reference, and demonstrates that electron delocalization in the excited state can be leveraged for artificial photosynthesis or other photocatalytic schemes based on electron transfer chemistry.

## Introduction

Solar energy conversion and photocatalysis intensively exploit excited-state chemical processes.[1–3] Intra/intermolecular excited-state electron transfer chemistry stands out as one of the basic steps in complex sequences that follow photon absorption.[4] It pertains to photosynthetic schemes, where it drives the chemical potential of the absorbed energy to the reaction centers and prepares solar fuels, to photovoltaic devices, where it injects electrons in photoelectrodes, and to a multitude photoredox catalytic reactions that allow to obtain fine chemicals. However, a prototypical model of intramolecular *excited-sate* electron transfer has not yet been established.

The prototypical model for intramolecular *ground-state* electron transfer is the Creutz–Taube ion, $[(NH_3)_5Ru^{II}(\mu\text{-pz})Ru^{III}(NH_3)_5]^{5+}$ ($\mathbf{CT}^{5+}$, where pz = pyrazine, Scheme 1),[5] which gave rise to the field of molecular mixed valency and became a hallmark of electron transfer research.[6,7] Mixed valence (MV) systems are those where the same chemical fragment is present in two formally different oxidation states.[8–12] In $\mathbf{CT}^{5+}$, a $Ru^{II}$ and a $Ru^{III}$ metal ion constitute a MV core with a $d\pi^6$-$d\pi^5$ electronic configuration. MV systems offer a unique playground for chemists to study the fundamentals of intramolecular electron transfer under a variety of different conditions. Systematic variations of temperature,[13] pressure,[14] solvent identity,[15,16] redox-active site potentials[17–19] and bridges connecting those redox sites[12,20–22] are usually translated into clear experimental observables. Therefore MV systems in general, and the prototypical $\mathbf{CT}^{5+}$ ion in particular, serve as models for how those variations affect electron transfer reactions. One of

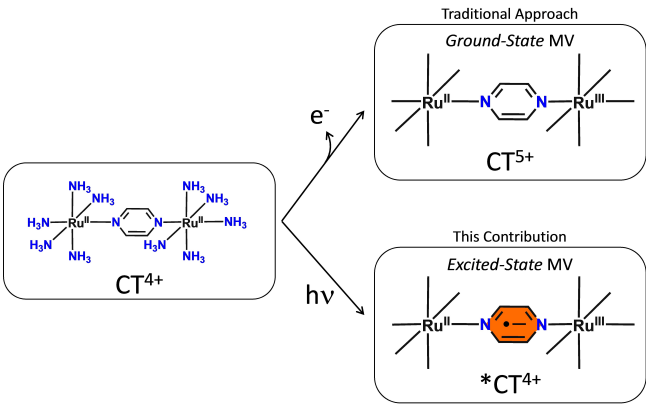


***Scheme 1.*** Sketches of the Creutz–Taube ion ($\mathbf{CT}^{5+}$), its one-electron reduced form ($\mathbf{CT}^{4+}$), and the excited-state Creutz–Taube ion ($*\mathbf{CT}^{4+}$).

[*] Dr. G. E. Pieslinger, I. Ramírez-Wierzbicki, Dr. A. Cadranel
Universidad de Buenos Aires, Facultad de Ciencias Exactas y Naturales, Departamento de Química Inorgánica, Analítica y Química Física,
Pabellón 2, Ciudad Universitaria, C1428EHA, Buenos Aires (Argentina)
E-mail: acadranel@qi.fcen.uba.ar
Dr. G. E. Pieslinger
CONICET—Universidad de Buenos Aires, Instituto de Química y Fisicoquímica Biológicas (IQUIFIB)
Junín 956, C1113AAD, Buenos Aires (Argentina)
I. Ramírez-Wierzbicki, Dr. A. Cadranel
CONICET—Universidad de Buenos Aires, Instituto de Química Física de Materiales, Medio Ambiente y Energía (INQUIMAE)
Pabellón 2, Ciudad Universitaria, C1428EHA, Buenos Aires (Argentina)
Dr. A. Cadranel
Department Chemie und Pharmazie, Physikalische Chemie, Friedrich-Alexander-Universität Erlangen-Nürnberg
Egerlandstraße 3, 91058 Erlangen (Germany)
E-mail: ale.cadranel@fau.de

the most striking features of MV systems is their intervalence charge transfer (IVCT) absorption, a process in which photon absorption is accompanied by an electron transfer from the formally reduced site to the formally oxidized site within the MV core. The IVCT band characteristics can be related to the thermal pathways of electron transfer.[23] In addition to the basic interest in electron transfer itself, applied research on mixed valency deals with charge delocalization and charge transport along molecular junctions. The target is to achieve molecular wire behavior and to implement such molecular materials in molecular electronics.[24–29]

More than fifty years after the appearance of the $\mathbf{CT}^{5+}$ ion, research on this field is still very active,[30–39] but has been primarily focused on ground-state mixed valence (GSMV) systems. This has been favored by the experimental accessibility of IVCT absorptions, on one hand, and ground state redox potentials, which are an additional key feature that allow to characterize electronic communication between the redox sites,[40] on the other hand. Additionally, time-resolved spectroscopic techniques have been applied to study GSMV systems upon excitation in their IVCT band.[41–50] However, the advent of robust and sensitive ultrafast transient absorption techniques with broad band detection (especially in the NIR) has also promoted investigations in a different type of MV systems, which are not MV systems in their ground states. In such photoinduced mixed valence (PIMV) systems, MV fragments are created only upon absorption of a photon,[51–56] and photoinduced intervalence charge transfer (PIIVCT) bands are observed only in the excited state.[57–59] Therefore, PIMV systems are prototypical models for intramolecular *excited-state* electron transfer. In fact, many reported bimetallic coordination complexes involve excited states that are PIMV systems, like MLCT states in $Cu^{I}$–$Cu^{II}$[60–62] or MMLCT states in $Pt^{II}$–$Pt^{II}$[63–65] compounds, but this has been rarely pointed out or analyzed in detail. Furthermore, PIMV systems can be potentially incorporated into molecular electronics, where light inputs drive controlled changes in molecular conductivity, similar to what happens in photo-switchable mixed valence systems.[66]

With this in mind, we sought to prepare an excited state analog of the $\mathbf{CT}^{5+}$ ion. To this end, we started with $[(NH_3)_5Ru^{II}(\mu\text{-pz})Ru^{II}(NH_3)_5]^{4+}$ ($\mathbf{CT}^{4+}$, Scheme 1) as a precursor. In $\mathbf{CT}^{4+}$, both ruthenium ions are $Ru^{II}$, and therefore it can be described as a $d\pi^6$-$d\pi^6$ bimetallic complex. Visible light excitation prepares $^*\mathbf{CT}^{4+}$. There, a negative charge from the bimetallic core is transferred to the pyrazine bridge, populating a manifold of metal to bridge charge transfer (MBCT) excited states. Thus, this process generates a transient mixed valence core with a $d\pi^6$-$d\pi^5$ electronic configuration bridged by a pyrazine radical anion, i.e., an *excited-state* CT ion. In this contribution, we investigate the absorption features and the dynamics of the MBCT states of this PIMV system by means of femtosecond transient absorption spectroscopy (fsTAS) using vis-NIR broadband detection. These experiments were complemented with DFT and (TD)DFT calculations, that help to understand the spectroscopy and electronic structure of the excited-state CT ion. Altogether, the PIMV system $^*\mathbf{CT}^{4+}$ is a model for intramolecular *excited-state* electron transfer and will serve as a cornerstone for systematic studies.

## Results and Discussion

The vis-NIR absorption spectrum of $\mathbf{CT}^{4+}$ in $D_2O$ is shown in Figure 1. It is governed by a rather intense MBCT band, from ruthenium-centered dπ to pyrazine-centered π* orbitals. The maximum is located at 18200 $cm^{-1}$, with a molar extinction coefficient of 30000 $M^{-1}cm^{-1}$.[67] A simplified molecular orbital diagram was already reported (Figure S1),[15,68,69] which allows to understand the electronic spectroscopy. This model considers Ru-pz backbonding interactions that selectively stabilize the $b_{3u}$ and destabilize the $b_{2g}$ orbitals. The rather simple structure of this compound affords only one ligand orbital, $\pi^*_{pz}(b_{3u})$, to be involved in visible light absorption. The main contributions to the absorption band are known to originate in a $d_{Ru}(b_{2g})\rightarrow\pi^*_{pz}$ transition with minor contributions of $d_{Ru}$-$(nb)\rightarrow\pi^*_{pz}$ at slightly lower energy. The spectroscopic properties of several related compounds can be successfully described with this model.[15,68,70] Our spectroelectrochemical measurements upon one-electron oxidation of $\mathbf{CT}^{4+}$ in $D_2O$ to give $\mathbf{CT}^{5+}$ (Figure 1a) show that the intensity of the MBCT absorption decreases to 21000 $M^{-1}cm^{-1}$, in agreement with previous reports.[67] Furthermore, an intense

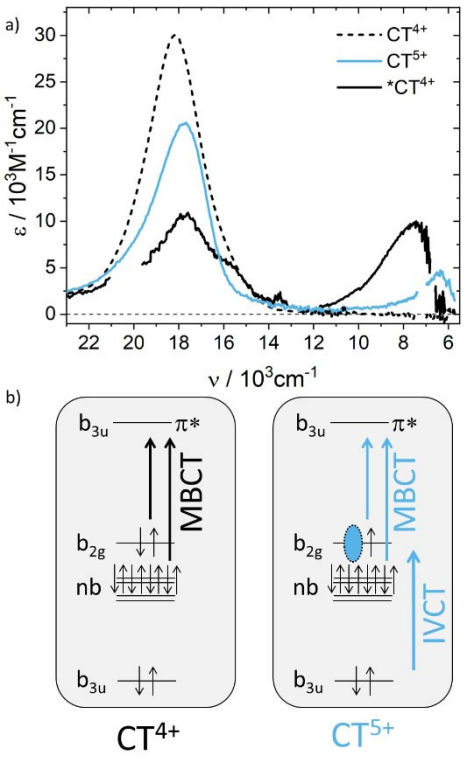


***Figure 1.*** a) vis-NIR absorption spectrum of $\mathbf{CT}^{4+}$, $\mathbf{CT}^{5+}$ and $^*\mathbf{CT}^{4+}$ in $D_2O$ at room temperature. b) orbital origin of the MBCT electronic transitions in $\mathbf{CT}^{4+}$, and IVCT electronic transitions in $\mathbf{CT}^{5+}$.

IVCT absorption appears at 6400 $cm^{-1}$. Both are a consequence of a semi-occupied $d_{Ru}(b_{2g})$ orbital, which is a worse donor for MBCT absorptions, and the acceptor of the IVCT absorptions.

With this information at hand, fsTAS studies were performed on $\mathbf{CT}^{4+}$ in $D_2O$ at room temperature, using 20000 $cm^{-1}$ (500 nm) excitation. Figure 2a shows the differential absorption spectra as a 3D map. Immediately after the pump pulse, the whole visible range is dominated by negative signals that indicate a loss of ground state population. These decay monotonically, indicating ground state recovery (Figure 2b). In the NIR range, a distinct photoinduced absorption appears around 7500 $cm^{-1}$. This is ascribed to the PIIVCT absorptions of the excited-state CT ion.[59,71] Multiwavelength global analysis reveals two exponential processes: a major component with a lifetime of 2.8 ns, and a minor component that lives 136 ps. A target model consisting of two parallelly decaying excited states was employed to fit the data.[72] The resulting species associated differential spectra are shown in Figure 2d, while the model applied is depicted in Figure 2c.[73] This model considers that laser excitation populates $^1$MBCT excited states, that intersystem cross to the triplet manifold in around 100 fs.[74,75] Then, intramolecular vibrational energy redistribution and vibrational cooling processes take place in an ultrafast timescale, which is beyond the resolution of our instrument. Therefore, our observations start with two different excited state populations, that are already relaxed and triplet in character. The longest lived excited state (black spectrum in Figure 2d) bears a bleach at 18200 $cm^{-1}$, and an intense PIIVCT at 7500 $cm^{-1}$,[59,71] whose orbital origin is the same than that one of the ground state IVCT band in $\mathbf{CT}^{5+}$, $d(b_{3u}) \rightarrow d(b_{2g})$ (Figure 2f).[15,68,76] In fact, the electronic configuration of $^3$MBCT($b_{2g}$) is identical to that one of $\mathbf{CT}^{5+}$, except for the additional excited electron in a pyrazine π* orbital in $*\mathbf{CT}^{4+}$. We therefore conclude that the $^3$MBCT($b_{2g}$) transient species is the excited-state analog of $\mathbf{CT}^{5+}$. Since $d(b_{2g})$ and $d(b_{3u})$ are combinations of the individual $d_{xz}$ orbitals (Figure S1), in $^3$MBCT($b_{2g}$) the excited hole is delocalized along the bimetallic core, and it can be described with a $\{Ru^{III-\delta}(\mu\text{-}pz^{\bullet-})Ru^{II+\delta}\}$ electronic configuration.

The intermediate lived excited state (orange spectrum in Figure 2d) includes a bleach at 18400 $cm^{-1}$, and weak and broad photoinduced absorptions to the red. This state is assigned as $^3$MBCT(nb), in which the excited hole sits in a d(nb) orbital (Figure 2f). Due to the absence of intense PIIVCT absorptions, the $^3$MBCT(nb) wave function can be considered localized, so this excited state can be described with a $\{Ru^{III}(\mu\text{-}pz^{\bullet-})Ru^{II}\}$ electronic configuration. In this picture, no PIIVCTs are expected because the $d(b_{2g})$ orbital is fully occupied. The weak and broad photoinduced absorptions that tail to the NIR probably have $d(b_{3u}) \rightarrow$ d(nb) contributions. $^3$MBCT(nb) can be regarded as an intraconfigurational mixed valence isomer of $^3$MBCT($b_{2g}$). According to this interpretation, $^3$MBCT(nb) is higher in energy than $^3$MBCT($b_{2g}$).

Next, theoretical calculations were employed to provide insights into the electronic structure of $*\mathbf{CT}^{4+}$. The lowest energy excited state was obtained via DFT optimization in the triplet potential energy surface of $\mathbf{CT}^{4+}$ (Table S1). This affords a spin density that is highly delocalized over the {Ru(μ-pz)Ru} core, with important contributions over the pyrazine bridge (Figure 3). The (TD)DFT calculated elec-

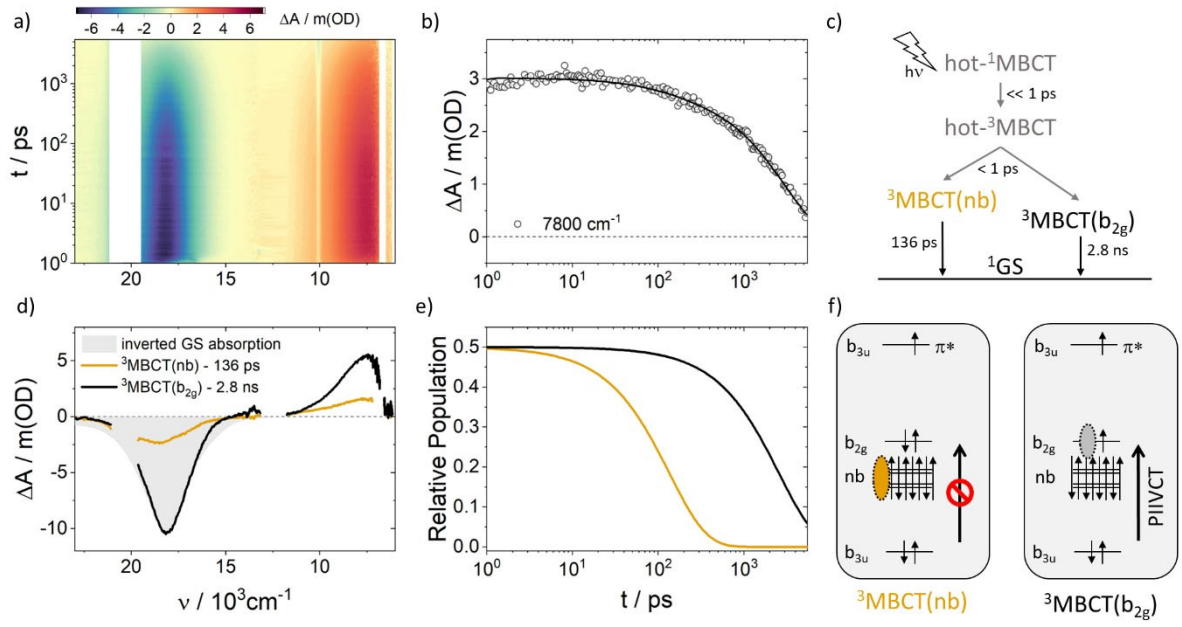


***Figure 2.*** a) Differential absorption 3D map obtained from fsTAS with 20000 $cm^{-1}$ excitation of $\mathbf{CT}^{4+}$ in $D_2O$ at room temperature (upper left). b) Differential absorption kinetic traces at 7500 $cm^{-1}$. c) Model employed to fit the data. d) Species associated differential spectra of $^3$MBCT($b_{2g}$) (black) and $^3$MBCT(nb) (orange). The inverted ground state absorption was also included (grey). e) Time evolution of the relative populations of $^3$MBCT($b_{2g}$) (black) and $^3$MBCT(nb) (orange). f) Orbital description of the different excited states and origin of the PIIVCT absorption.

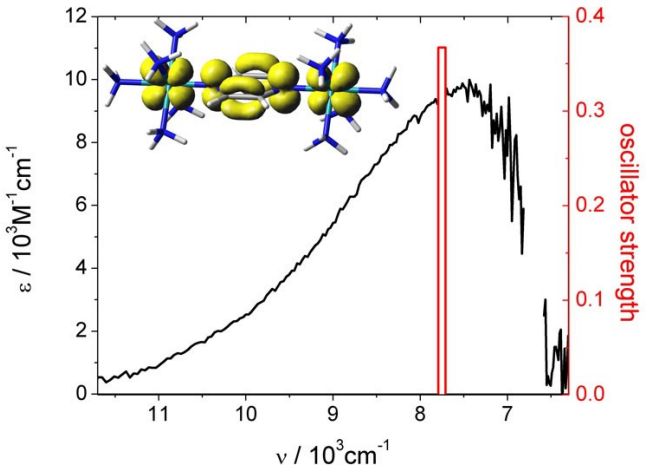


***Figure 3.*** Experimental photoinduced intervalence charge transfer (PIIVCT) band (black curve) and calculated electronic transitions (red bars) for the lowest triplet state $*\mathbf{CT}^{4+}$. The inset shows the calculated spin density map.

tronic absorption spectrum of the optimized triplet yields an electronic transition at 7754 $cm^{-1}$, in excellent agreement with the experimentally observed PIIVCT for $*\mathbf{CT}^{4+}$ (Figures 3 and S7, Table S2). As expected for a strongly delocalized configuration, the calculated electron density difference for this transition (Figure S8) reveals a π-π* rather than a charge transfer character. Furthermore, virtually identical spin densities and calculated electronic transitions are obtained upon scanning the dihedral angle between pyrazine and the *mer*-{$Ru(NH_3)_3$} plane from 0 to 45° (Table S3), and also upon scanning the dihedral angle between both *mer*-{$Ru(NH_3)_3$} moieties from 0 to 45° (Table S4).[77] Therefore, the calculated electronic structure is a very good description of the $^3MBCT(b_{2g})$ state.

Interestingly, the excited state band lies about 1300 $cm^{-1}$ higher than the ground state band, although $^3MBCT(b_{2g})$ and $\mathbf{CT}^{5+}$ share the same $d(b_{2g})$ configuration of the excited hole. The diabatic energy difference within the metal-metal donor-acceptor pair is not significantly affected by the excited electron on the bridge π* orbital, because both $^3MBCT(b_{2g})$ and $\mathbf{CT}^{5+}$ are symmetric systems. Therefore, the energy shift is a direct consequence of the increased electronic coupling.

The notorious asymmetry of the PIIVCT band with a low-energy skewing is a further indication of strong electronic coupling. Its full width at half maximum is 2200 $cm^{-1}$, larger than the 1400 $cm^{-1}$ observed for the ground state $\mathbf{CT}^{5+}$ (Table 1). Furthermore, like the ground state IVCT, the PIIVCT band is solvent independent (Figure S2). Strikingly, solvent independence is evident at time delays as short as 1 ps after excitation. This result is significative *per se* because it demonstrates that in the excited state the solvent is averaged in a very fast timescale ($10^{-12}$ s) after the PIIVCT absorption event ($10^{-14}$ s). DFT calculations also point to a strong electronic coupling, since Mulliken spin densities are calculated to be equally 0.65 for

***Table 1:*** Properties of the ground-state intervalence charge transfer (GSIVCT) and excited-state intervalence charge transfer (PIIVCT) bands in the ground state and in the excited state of $\mathbf{CT}^{5+}$ and $*\mathbf{CT}^{4+}$, respectively, in $D_2O$.

| Property | GSIVCT[80] | PIIVCT |
|---|---|---|
| $\nu$ [$cm^{-1}$] | 6400 | 7500 |
| $\varepsilon$ [$M^{-1}\,cm^{-1}$] | 5000 | 10500 |
| $\Delta\nu_{1/2}$ [$cm^{-1}$] | 1400 | 2200 |
| $H_{DA}$ [$cm^{-1}$] | 3300 | 3750 |
| Solvent Dependence | independent | independent |

each Ru ion, and a very intense PIIVCT transition is calculated.

All the aforementioned indicates that the excited-state Creutz–Taube ion is a MV system that belongs to Class II/III or Class III according to Robin, Day and Meyer.[7,78] In this context, the donor-acceptor electronic coupling element, $H_{DA}$, is best calculated[23] using $H_{DA}=\nu_{max}/2$, where $\nu_{max}$ is the energy of the PIIVCT maximum. $H_{DA}=3750\ cm^{-1}$ for $^3MBCT(b_{2g})$, 15 % higher than that for ground-state $\mathbf{CT}^{5+}$ (Table 1). The physical origin of the significant increase in $H_{DA}$ is not related to drastic structural changes that may accompany reduction of the pyrazine, like with 4,4′-bipyridine or other biphenyl bridging ligands.[79] Instead, the enhancement in $H_{DA}$ is probably a consequence of an increased number of virtual states (other MBCT states, MC states) that help in mixing donor-acceptor orbitals via superexchange interactions in the excited state. In related work,[59] a comparison of pz and $pz^{\bullet-}$ as bridging ligands in MV systems could only qualitatively conclude that they promoted similar electronic couplings. This conclusion was, however, of limited applicability, since the PIIVCT band was measured in a rigid polymeric matrix. The influences of this medium in reorganization energies resulted in a red shift of the PIIVCT against the ground state IVCT, opposite to what was observed here, obscuring a quantitative comparison. In fact, our study is the first quantitative determination of the electronic coupling of the excited-state Creutz–Taube ion in the same conditions than those utilized for the prototypical ground-state $\mathbf{CT}^{5+}$.

Notable are excited state lifetimes of $*\mathbf{CT}^{4+}$. To the best of our knowledge, $^3MBCT(b_{2g})$ in $*\mathbf{CT}^{4+}$ is the longest-lived excited state of mono-imine Ru complexes reported to date. $^3MLCT$ states in monomeric $[Ru(NH_3)_5(pz)]^{2+}$ and $[Ru(NH_3)_5(pzH)]^{3+}$ reference compounds live 225 ps and 25 ps, respectively.[70,81] This was interpreted in terms of activated population of MC states for $[Ru(NH_3)_5(pz)]^{2+}$ (Figure 4). For $[Ru(NH_3)_5(pzH)]^{3+}$, stabilization of the $^3MLCT$ due to protonation disfavored MC population, but also led to a highly coupled and barrierless $^3MLCT\rightarrow GS$ transition. In $*\mathbf{CT}^{4+}$, $^3MBCT$ states are also stabilized due to coordination of the second Ru ion in the distal N atom of pz. Nevertheless, strong electron delocalization nests the potential energy surface of $^3MBCT(b_{2g})$ with that of the ground state $\mathbf{CT}^{4+}$, and in consequence a poor Franck–Condon factor is involved in the $^3MBCT(b_{2g})\rightarrow GS$ transition. Actually, if electron delocalization is impeded as in $^3MBCT(nb)$, a situation similar to that of $[Ru(NH_3)_5(pzH)]^{3+}$ is observed.

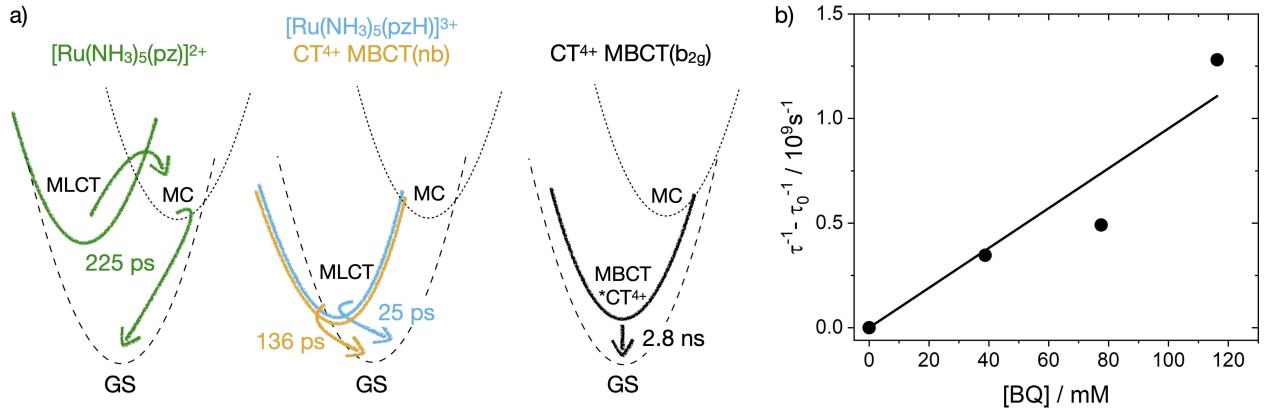


***Figure 4.*** a) ground- and excited-state potential energy surfaces that explain excited state lifetimes in $[Ru(NH_3)_5(pz)]^{2+}$ (green), $[Ru(NH_3)_5(pzH)]^{3+}$ (cyan), MBCT(nb) (orange) and MBCT($b_{2g}$) (black). b) Stern–Volmer analysis of bimolecular electron transfer between $*\mathbf{CT}^{4+}$ and BQ in DMF at room temperature.

Extension of excited state lifetimes by a factor of 2 thanks to hole delocalization has been previously observed.[53] But the $^3$MBCT($b_{2g}$) lifetime in $*\mathbf{CT}^{4+}$ of 2.8 ns is, strikingly, at least two orders of magnitude larger than that of $[Ru(NH_3)_5(pzH)]^{3+}$, fully leveraging delocalization effects. In fact, this allows $*\mathbf{CT}^{4+}$ to enter the arena of excited state bimolecular reactivity, illustrating the importance of excited-state mixed valence systems.

The nanosecond lifetime of $*\mathbf{CT}^{4+}$ was exploited for bimolecular electron transfer, a key reaction in photocatalysis and energy conversion, with benzoquinone (BQ) as an electron acceptor in DMF [Eq. (1)].

$$Ru^{III-\delta}(\mu pz^{\bullet-})Ru^{II+\delta} + BQ \rightarrow Ru^{III-\delta}(\mu pz)Ru^{II+\delta} + BQ^{\bullet-} \quad (1)$$

$$Ru^{III-\delta}(\mu pz)Ru^{II+\delta} + BQ^{\bullet-} \rightarrow Ru^{II}(\mu pz)Ru^{II} + BQ \quad (2)$$

$^3$MBCT($b_{2g}$) lifetimes were observed to decrease upon increasing BQ concentrations (Figures S3–S6). A Stern–Volmer analysis (Figure 4b) afforded a bimolecular quenching constant of $(9\pm1)\times10^9\ M^{-1}s^{-1}$, consistent with diffusion-controlled processes. No evidence of the charge separated state formed, consisting of $BQ^{\bullet-}$ and $\mathbf{CT}^{5+}$ [Eq. (1)], was observed. This implies that charge recombination by means of back electron transfer [Eq. (2)] is faster than forward electron transfer, impeding accumulation and detection of the charge-separated products. Further experiments concerning the influence of intramolecular electron transfer (electron delocalization) in intermolecular electron transfer reactions are underway in our labs.

## Conclusion

The excited-state Creutz–Taube ion $*\mathbf{CT}^{4+}$ has been prepared and characterized. The electronic configuration was determined to be analogous to that of the ground-state Creutz–Taube ion $\mathbf{CT}^{5+}$, with photoinduced IVCT absorptions originating in $d(b_{3u}) \rightarrow d(b_{2g})$ transitions. Electronic coupling in the excited state is very strong, and higher than in the ground state due to a multitude of excited states that participate in the super-exchange interactions. An immediate consequence of electron delocalization is the extension of excited state lifetimes of $*\mathbf{CT}^{4+}$ by two orders of magnitude, which was leveraged in proof-of-concept bimolecular reactions with a benzoquinone acceptor. Thus, a reference for photoinduced mixed valence systems and intramolecular excited-state electron transfer is established.

## Acknowledgements

IRW is a doctoral fellow of UBA. GEP and AC are members of the research staff of CONICET and AC is a fellow of ALN. Funding from CONICET (PIP 11220200102757CO) and ANPCyT (PICT 2018–00924 and 2019–02410) is acknowledged. AC thanks Dirk Guldi for providing access to transient spectroscopic facilities. GEP thanks Prof. Dr. Adrián Roitberg for selflessly sharing his knowledge. Open Access funding enabled and organized by Projekt DEAL.

## Conflict of Interest

The authors declare no conflict of interest.

## Data Availability Statement

The data that support the findings of this study are available from the corresponding author upon reasonable request.

**Keywords:** Electron Transfer · Electronic Coupling · Excited States · Intervalence · Mixed Valence

[1] H. J. Sayre, L. Tian, M. Son, S. M. Hart, X. Liu, D. M. Arias-Rotondo, B. P. Rand, G. S. Schlau-Cohen, G. D. Scholes, *Energy Environ. Sci.* **2021**, *14*, 1402–1419.

[2] D. L. Ashford, M. K. Gish, A. K. Vannucci, M. K. Brennaman, J. L. Templeton, J. M. Papanikolas, T. J. Meyer, *Chem. Rev.* **2015**, *115*, 13006–13049.
[3] M. G. Pfeffer, C. Müller, E. T. E. Kastl, A. K. Mengele, B. Bagemihl, S. S. Fauth, J. Habermehl, L. Petermann, M. Wächtler, M. Schulz, D. Chartrand, F. Laverdière, P. Seeber, S. Kupfer, S. Gräfe, G. S. Hanan, J. G. Vos, B. Dietzek-Ivanšić, S. Rau, *Nat. Chem.* **2022**, *14*, 500–506.
[4] R. A. Marcus, N. Sutin, *Biochim. Biophys. Acta Rev. Bioenerg.* **1985**, *811*, 265–322.
[5] C. Creutz, H. Taube, *J. Am. Chem. Soc.* **1969**, *91*, 3988–3989.
[6] D. E. Richardson, H. Taube, *Coord. Chem. Rev.* **1984**, *60*, 107–129.
[7] K. D. Demadis, C. M. Hartshorn, T. J. Meyer, *Chem. Rev.* **2001**, *101*, 2655–2686.
[8] C. G. Young, *Coord. Chem. Rev.* **1989**, *96*, 89–251.
[9] P. Day, N. S. Hush, R. J. H. Clark, *Philos. Trans. R. Soc. A* **2008**, *366*, 5–14.
[10] J. P. Fackler, in *Encycl. Inorg. Bioinorg. Chem.*, Wiley, Chichester, **2011**.
[11] J. Hankache, O. S. Wenger, *Chem. Rev.* **2011**, *111*, 5138–5178.
[12] D. M. D'Alessandro, F. R. Keene, *Chem. Rev.* **2006**, *106*, 2270–2298.
[13] J. T. Hupp, G. A. Neyhart, T. J. Meyer, E. M. Kober, *J. Phys. Chem.* **1992**, *96*, 10820–10830.
[14] M. Dürr, J. Klein, A. Kahnt, S. Becker, R. Puchta, B. Sarkar, I. Ivanović-Burmazović, *Inorg. Chem.* **2017**, *56*, 14912–14925.
[15] C. Creutz, M. H. Chou, *Inorg. Chem.* **1987**, *26*, 2995–3000.
[16] K. S. Schanze, G. A. Neyhart, T. J. Meyer, *J. Phys. Chem.* **1986**, *90*, 2182–2193.
[17] A. Cadranel, P. Alborés, S. Yamazaki, V. D. Kleiman, L. M. Baraldo, *Dalton Trans.* **2012**, *41*, 5343–5350.
[18] A. Cadranel, B. M. Aramburu Trošelj, S. Yamazaki, P. Alborés, V. D. Kleiman, L. M. Baraldo, *Dalton Trans.* **2013**, *42*, 16723–16732.
[19] P. S. Oviedo, G. E. Pieslinger, A. Cadranel, L. M. Baraldo, *Dalton Trans.* **2017**, *46*, 15757–15768.
[20] P. Aguirre-Etcheverry, D. O'Hare, *Chem. Rev.* **2010**, *110*, 4839–4864.
[21] Y. Y. Yang, X. Q. Zhu, J. P. Launay, C. Bin Hong, S. D. Su, Y. H. Wen, X. T. Wu, T. L. Sheng, *Angew. Chem. Int. Ed.* **2021**, *60*, 4804–4814; *Angew. Chem.* **2021**, *133*, 4854–4864.
[22] J. P. Launay, *Chem. Soc. Rev.* **2001**, *30*, 386–397.
[23] B. S. Brunschwig, C. Creutz, N. Sutin, *Chem. Soc. Rev.* **2002**, *31*, 168–184.
[24] P. J. Low, *Dalton Trans.* **2005**, 2821–2824.
[25] O. A. Al-Owaedi, D. C. Milan, M. C. Oerthel, S. Bock, D. S. Yufit, J. A. K. Howard, S. J. Higgins, R. J. Nichols, C. J. Lambert, M. R. Bryce, P. J. Low, *Organometallics* **2016**, *35*, 2944–2954.
[26] D. Bu, Y. Xiong, Y. N. Tan, M. Meng, P. J. Low, D. Bin Kuang, C. Y. Liu, *Chem. Sci.* **2018**, *9*, 3438–3450.
[27] M. Naher, S. Bock, Z. M. Langtry, K. M. O'Malley, A. N. Sobolev, B. W. Skelton, M. Korb, P. J. Low, *Organometallics* **2020**, *39*, 4667–4687.
[28] S. Rigaut, *Dalton Trans.* **2013**, *42*, 15859–15863.
[29] M. D. Ward, *Chem. Soc. Rev.* **1995**, *24*, 121–134.
[30] A. D. P. Harrison, R. Grotjahn, M. Naher, M. Seyed, B. H. Ghazvini, D. M. Mazzucato, M. Korb, A. Moggach, C. Lambert, M. Kaupp, P. J. Low, *Angew. Chem. Int. Ed.* **2022**, *61*, e202211000; *Angew. Chem.* **2022**, *134*, e202211000.
[31] G. Y. Zhu, Y. Qin, M. Meng, S. Mallick, H. Gao, X. Chen, T. Cheng, Y. N. Tan, X. Xiao, M. J. Han, M. F. Sun, C. Y. Liu, *Nat. Commun.* **2021**, *12*, 456.
[32] F. Glaab, J. G. Wehner, C. Lambert, V. Engel, *J. Phys. Chem. A* **2019**, *123*, 5463–5471.
[33] F. F. Khan, S. Mondal, S. Chandra, N. I. Neuman, B. Sarkar, G. K. Lahiri, *Dalton Trans.* **2021**, *50*, 1106–1118.
[34] M. Krug, M. Wagner, T. A. Schaub, W. Zhang, C. M. Schüßlbauer, J. D. R. Ascherl, P. W. Münich, R. R. Schröder, F. Gröhn, P. O. Dral, M. Barbatti, D. M. Guldi, M. Kivala, *Angew. Chem. Int. Ed.* **2020**, *59*, 16233–16240; *Angew. Chem.* **2020**, *132*, 16368–16376.
[35] J. M. Palasz, T. M. Porter, C. P. Kubiak, *Inorg. Chem.* **2020**, *59*, 10532–10539.
[36] O. Impert, A. Kozakiewicz, G. Wrzeszcz, A. Katafias, A. Bieńko, R. van Eldik, A. Ozarowski, *Inorg. Chem.* **2020**, *59*, 8609–8619.
[37] M. Y. Livshits, L. Wang, S. B. Vittardi, S. Ruetzel, A. King, T. Brixner, J. J. Rack, *Chem. Sci.* **2020**, *11*, 5797–5807.
[38] L. Đorđević, C. Valentini, N. Demitri, C. Mézière, M. Allain, M. Sallé, A. Folli, D. Murphy, S. Mañas-Valero, E. Coronado, D. Bonifazi, *Angew. Chem. Int. Ed.* **2020**, *59*, 4106–4114; *Angew. Chem.* **2020**, *132*, 4135–4143.
[39] P. W. Doheny, J. K. Clegg, F. Tuna, D. Collison, C. J. Kepert, D. M. D'Alessandro, *Chem. Sci.* **2020**, *11*, 5213–5220.
[40] R. F. Winter, *Organometallics* **2014**, *33*, 4517–4536.
[41] C. Liekhus-Schmaltz, Z. W. Fox, A. Andersen, K. S. Kjaer, R. Alonso-Mori, E. Biasin, J. Carlstad, M. Chollet, J. D. Gaynor, J. M. Glownia, K. Hong, T. Kroll, J. H. Lee, B. I. Poulter, M. Reinhard, D. Sokaras, Y. Zhang, G. Doumy, A. M. March, S. H. Southworth, S. Mukamel, A. A. Cordones, R. W. Schoenlein, N. Govind, M. Khalil, *J. Phys. Chem. Lett.* **2022**, *13*, 378–386.
[42] E. Biasin, Z. W. Fox, A. Andersen, K. Ledbetter, K. S. Kjær, R. Alonso-Mori, J. M. Carlstad, M. Chollet, J. D. Gaynor, J. M. Glownia, K. Hong, T. Kroll, J. H. Lee, C. Liekhus-Schmaltz, M. Reinhard, D. Sokaras, Y. Zhang, G. Doumy, A. M. March, S. H. Southworth, S. Mukamel, K. J. Gaffney, R. W. Schoenlein, N. Govind, A. A. Cordones, M. Khalil, *Nat. Chem.* **2021**, *13*, 343–349.
[43] S. D. Su, X. Q. Zhu, L. T. Zhang, Y. Y. Yang, Y. H. Wen, X. T. Wu, S. Q. Yang, T. L. Sheng, *Dalton Trans.* **2019**, *48*, 9303–9309.
[44] C. Lambert, M. Moos, A. Schmiedel, M. Holzapfel, J. Schäfer, M. Kess, V. Engel, *Phys. Chem. Chem. Phys.* **2016**, *18*, 19405–19411.
[45] J. B. G. Gluyas, A. N. Sobolev, E. G. Moore, P. J. Low, *Organometallics* **2015**, *34*, 3923–3926.
[46] A. Heckmann, S. Dümmler, J. Pauli, M. Margraf, J. Köhler, D. Stich, C. Lambert, I. Fischer, U. Resch-Genger, *J. Phys. Chem. C* **2009**, *113*, 20958–20966.
[47] R. Maksimenka, M. Margraf, J. Köhler, A. Heckmann, C. Lambert, I. Fischer, *Chem. Phys.* **2008**, *347*, 436–445.
[48] B. P. Macpherson, P. V. Bernhardt, A. Hauser, S. Pagès, E. Vauthey, *Inorg. Chem.* **2005**, *44*, 5530–5536.
[49] D. F. Watson, H. S. Tan, E. Schreiber, C. J. Mordas, A. B. Bocarsly, *J. Phys. Chem. A* **2004**, *108*, 3261–3267.
[50] D. H. Son, P. Kambhampati, T. W. Kee, P. F. Barbara, *J. Phys. Chem. A* **2002**, *106*, 4591–4597.
[51] E. A. Plummer, J. I. Zink, *Inorg. Chem.* **2006**, *45*, 6556–6558.
[52] C. Lambert, R. Wagener, J. H. Klein, G. Grelaud, M. Moos, A. Schmiedel, M. Holzapfel, T. Bruhn, *Chem. Commun.* **2014**, *50*, 11350–11353.
[53] B. M. Aramburu-Trošelj, P. S. Oviedo, G. E. Pieslinger, J. H. Hodak, L. M. Baraldo, D. M. Guldi, A. Cadranel, *Inorg. Chem.* **2019**, *58*, 10898–10904.
[54] B. M. Aramburu-Trošelj, P. S. Oviedo, I. Ramírez-Wierzbicki, L. M. Baraldo, A. Cadranel, *Chem. Commun.* **2019**, *55*, 7659–7662.
[55] J. Henderson, C. P. Kubiak, *Inorg. Chem.* **2014**, *53*, 11298–11306.

[56] J. F. Endicott, Y. J. Chen, *Inorg. Chim. Acta* **2007**, *360*, 913–922.
[57] D. M. Dattelbaum, C. M. Hartshorn, T. J. Meyer, *J. Am. Chem. Soc.* **2002**, *124*, 4938–4939.
[58] D. M. Dattelbaum, E. M. Kober, J. M. Papanikolas, T. J. Meyer, *Chem. Phys.* **2006**, *326*, 71–78.
[59] C. N. Fleming, D. M. Dattelbaum, D. W. Thompson, A. Y. Ershov, T. J. Meyer, *J. Am. Chem. Soc.* **2007**, *129*, 9622–9630.
[60] J. F. Nierengarten, I. Nierengarten, M. Holler, A. Sournia-Saquet, B. Delavaux-Nicot, E. Leoni, F. Monti, N. Armaroli, *Eur. J. Inorg. Chem.* **2019**, 2665–2673.
[61] C. Li, W. Li, A. F. Henwood, D. Hall, D. B. Cordes, A. M. Z. Slawin, V. Lemaur, Y. Olivier, I. D. W. Samuel, E. Zysman-Colman, *Inorg. Chem.* **2020**, *59*, 14772–14784.
[62] A. N. Desnoyer, A. Nicolay, P. Rios, M. S. Ziegler, T. D. Tilley, *Acc. Chem. Res.* **2020**, *53*, 1944–1956.
[63] B. Ma, J. Li, P. I. Djurovich, M. Yousufuddin, R. Bau, M. E. Thompson, *J. Am. Chem. Soc.* **2005**, *127*, 28–29.
[64] B. Ma, P. I. Djurovich, S. Garon, B. Alleyne, M. E. Thompson, *Adv. Funct. Mater.* **2006**, *16*, 2438–2446.
[65] M. Chaaban, C. Zhou, H. Lin, B. Chyi, B. Ma, *J. Mater. Chem. C* **2019**, *7*, 5910–5924.
[66] O. S. Wenger, *Chem. Soc. Rev.* **2012**, *41*, 3772–3779.
[67] C. Creutz, H. Taube, *J. Am. Chem. Soc.* **1973**, *95*, 1086–1094.
[68] J. W. Lauher, *Inorg. Chim. Acta* **1980**, *39*, 119–123.
[69] K. Neuenschwander, S. B. Piepho, P. N. Schatz, *J. Am. Chem. Soc.* **1985**, *107*, 7862–7869.
[70] J. R. Winkler, T. L. Netzel, C. Creutz, N. Sutin, *J. Am. Chem. Soc.* **1987**, *109*, 2381–2392.
[71] I. Ramírez-Wierzbicki, A. Cotic, A. Cadranel, *ChemPhysChem* **2022**, *e202200384, DOI: 10.1002/cphc.202200384*.
[72] P. S. Oviedo, G. E. Pieslinger, L. M. Baraldo, A. Cadranel, D. M. Guldi, *J. Phys. Chem. C* **2019**, *123*, 3285–3291.
[73] An all-sequential model results in very similar differential spectra for both species. However, this lacks any physicochemical meaning since the first process is too slow to correspond to vibrational cooling within the same electronic configuration.
[74] N. H. Damrauer, G. Cerullo, A. Yeh, T. R. Boussie, C. V. Shank, J. K. McCusker, *Science* **1997**, *275*, 54–57.
[75] M. Chergui, *Dalton Trans.* **2012**, *41*, 13022.
[76] S. B. Piepho, *J. Am. Chem. Soc.* **1990**, *112*, 4197–4206.
[77] M. Parthey, J. B. G. Gluyas, M. A. Fox, P. J. Low, M. Kaupp, *Chem. Eur. J.* **2014**, *20*, 6895–6908.
[78] M. B. Robin, P. Day, *Adv. Inorg. Chem. Radiochem.* **1968**, *10*, 247–422.
[79] A. Cotic, S. Cerfontaine, L. D. Slep, B. Elias, L. Troian-Gautier, A. Cadranel, *Phys. Chem. Chem. Phys.* **2022**, *24*, 15121–15128.
[80] C. Creutz, *Prog. Inorg. Chem.* **1983**, *30*, 1–73.
[81] C. Creutz, P. Kroger, T. Matsubara, T. L. Netzel, N. Sutin, *J. Am. Chem. Soc.* **1979**, *101*, 5442–5444.

Manuscript received: August 10, 2022
Accepted manuscript online: September 26, 2022
Version of record online: October 18, 2022